Olefin Metathesis–Based Chemically Recyclable Polymers Enabled by a Fused-Ring Monomer

Junpeng Wang (jwang6@uakron.edu)
University of Akron
Devavrat Sathe
University of Akron
Junfeng Zhou
University of Akron https://orcid.org/0000-0002-8201-6799
Hanlin Chen
University of Akron
Hsin-Wei Su
University of Akron
Wei Xie
University of Akron
Tze-Gang Hsu
University of Akron
Briana Schrage
University of Akron
Travis Smith
University of Akron
Christopher Ziegler
University of Akron

Article

Keywords: Plastics Sustainability, Thermal Stability, Tunable Mechanical Properties

Posted Date: October 6th, 2020

DOI: https://doi.org/10.21203/rs.3.rs-82630/v1

Version of Record: A version of this preprint was published at Nature Chemistry on July 22nd, 2021. See the published version at https://doi.org/10.1038/s41557-021-00748-5.

Abstract

A promising solution to address the challenges in plastics sustainability is to replace current polymers with chemically recyclable ones that can depolymerise into their constituent monomers for circular use of materials. Despite the progress, few depolymerisable polymers exhibit the excellent thermal stability and strong mechanical properties of traditional polymers. Here we report a series of chemically recyclable polymers that show excellent thermal stability (decomposition temperature > 370 ºC) and tunable mechanical properties. The polymers are formed via ring-opening metathesis polymerisation of cyclooctene with a trans-cyclobutane installed at the 5,6-positions. The additional ring converts the non-depolymerisable polycyclooctene into a depolymerisable polymer by reducing the ring strain energy in the monomer (from 8.2 kcal/mol in unsubstituted cyclooctene to 4.9 kcal/mol in the fused ring). The fused-ring monomer enables a broad scope of functionalities to be incorporated, providing access to chemically recyclable elastomers and plastics that show promise as next-generation sustainable materials.

Main Text

Synthetic polymers, including synthetic rubber and synthetic plastics, have been used in nearly every aspect of our daily lives. The dominance of synthetic polymers is largely driven by their excellent stability and processability as well as their versatile mechanical properties. However, due to their high durability, waste materials composed of these polymers have accumulated in the ocean and have caused serious concerns for marine ecosystems[1]. In addition, since 90% of these polymers are derived from finite fossil feedstocks, the production of these materials is unsustainable if they cannot be recycled and reused[2]. Efforts to address these issues include the development of biodegradable polymers and mechanical recycling. However, most biodegradable polymers that can be degraded in artificial environments do not undergo efficient degradation in seawater, giving rise to new environmental consequences[3]. Mechanical recycling of polymers typically results in significant loss of quality, and the recycled material is not suitable for high-performance applications[4]. A particularly attractive strategy is to develop chemically recyclable polymers that can be depolymerised into their constituent monomers for recycling and repolymerisation[5,6]. Circular use of the materials will not only help to preserve finite natural resources but can also address the end-of-life issues.

To replace currently available commercial polymers, depolymerisable polymers need to match or exceed the properties of the current ones. With exceptions, polymerisation is typically favored in enthalpy ($\Delta H < 0$) and disfavored in entropy ($\Delta S < 0$). The temperature at which the entropic loss will offset the enthalpic gain is defined as the ceiling temperature T_c, and depolymerisation is favored when the temperature is above T_c. Common polymers such as polyolefins have high T_c's, and their depolymerisation is either costly in terms of energy or is susceptible to decomposition. Classical low-T_c polymers such as poly(olefin sulfone)s[7,8], poly(*α*-methyl styrene)[9], and polyaldehydes[10] lack high thermal and chemical stability, and their use has been limited to certain specific applications such as transient electronics[11–13]. A promising strategy to address both the stability issues is to develop polymers that only undergo efficient

depolymerisation in the presence of a catalyst. In other words, without the catalyst, the polymer is in a kinetic trap so that it will stay intact even when the temperature is above T_c. Recently, it has been shown that ring-opening polymerisation of certain cyclic monomers—such as cyclic esters, cyclic carbonates and cyclic olefins—can lead to polymers that can depolymerise into the corresponding monomers in the presence of catalysts but show high thermal stability when the catalysts are removed[6]. For example, Chen and coworkers have shown that a poly(γbutyrolactone) required heating overnight at 300 ºC to be depolymerised, but the depolymerisation temperature was reduced to 120 ºC when a $ZnCl_2$ catalyst was added[14].

Among the catalytically depolymerisable polymers, a particularly attractive system is the one that is based on olefin metathesis[15]. Since olefin metathesis does not occur without a catalyst, unintended depolymerisation can be prevented when the catalyst is removed. In addition, metathesis is compatible with a wide variety of functional groups and can be conducted in mild or ambient reaction conditions[15]. Metathesis-based depolymerisable polymers are typically made via ring-opening metathesis polymerisation (ROMP)[16] of cycloalkenes and can depolymerise through ring-closing metathesis (RCM)[17] to form the corresponding monomers. Compared to the ring-opening polymerisation that is based on cyclic esters and cyclic carbonates, ROMP allows the production of polymers with hydrocarbon backbones, which have greater hydrolytic and thermal stability. However, up to now, demonstrations of depolymerisable ROMP polymers have been limited to polymers of five-membered cycloalkenes, namely the polypentenamers[18]. As polypentenamers are typically amorphous polymers with glass transition temperatures (T_g's) below or near room temperature[18], they are not suitable for plastics applications where glassy or semicrystalline polymers are needed. Furthermore, the controlled polymerisation of cyclopentene is challenging: the reported cases of controlled polymerisation of cyclopentene either require that the conversion be limited to a low threshold (< 20%)[19] or need to be conducted in a variable-temperature fashion[20].

To address the needs for more robust depolymerisable ROMP polymers, we looked into other cyclic olefins. Since cyclopropene and cyclobutene are highly strained, with reported ring strain energies (RSEs) of 54.5 and 30.6 kcal/mol, respectively[21], the depolymerisation of their ROMP polymers is not feasible. The ring strain of cyclohexene is too low to achieve a successful ROMP [22]. Of the 7- to 12-membered cyclic olefins, the 8-membered one is particularly attractive because functionalized cyclooctenes can be made from 1,5-cyclooctadiene, an inexpensive, commercially available material. As a result, poly(cyclooctenes) have been one of the most extensively employed poly(cycloalkenes)[23]. In addition, the *Z*-alkene in cyclooctene can be inverted into an *E*-alkene to increase the ring strain energy (the RSE of *trans*-alkene cyclooctene is 16 kcal/mol[21]) and enable living polymerisation[24,25]. However, compared to cyclopentene (RSE = 5.2 kcal/mol), the higher ring strain of cyclooctene (RSE = 8.2 kcal/mol) precludes the depolymerisation of polycyclooctene[26]. We hypothesized that if the RSE of cyclooctene could be reduced to a level comparable to that of cyclopentene, the corresponding polymer would undergo similar depolymerisation.

It has been shown that the ring strain of cyclooctene can be lowered by a fused ring at the 5,6-positions and that the stereochemistry of the fused ring plays a critical role. For example, Coates and coworkers showed that an imidazolium-fused cyclooctene monomer only afforded macrocyclic oligomers under typical ROMP conditions, suggesting that the imidazolium-fused ring lowers the ring strain of cyclooctene[27]. Scherman *et al*. showed that a cyclooctene monomer with a *trans*-fused acetonide afforded much lower yield in polymerisation than a *cis*-acetonide cyclooctene monomer (15% vs. 80% when the polymerisation was conducted at 1.0 M monomer concentration), indicating that the *trans*-fused acetonide cyclooctene has a lower RSE than that of its *cis* analogue[28]. These studies suggest that an appropriate fused ring may lower the ring strain of cyclooctene to enable the depolymerisation of the corresponding ROMP polymer (Fig. 1A).

To identify a fused ring that can lower the ring strain of cyclooctene to the abovementioned target, we calculated the RSEs of cyclooctenes with 3-, 4-, 5-, and 6-membered rings fused at the 5,6-positions, including both *cis* and *trans* isomers (Fig. 1B). The computation of RSE was conducted by calculating the enthalpy change of the following RCM reaction (Eq. 1) using density functional theory (DFT) at the B3LYP/6-31G(d,p) level, which provided reasonable predictions for the RSEs of cyclic olefins[22].

(1)

Based on the difference in RSE between the fused rings and the unsubstituted cyclooctene (RSE = 8.2 kcal/mol), the calculated results can be sorted into three groups:

1. RSEs that are higher than that of the virgin cyclooctene, including *cis*-cyclopropane–, *trans*-cyclopropane–, and *cis*-cyclobutane–fused cyclooctenes;
2. Fused rings with slightly decreased ring strain, including
3. *cis*-cyclopentane–, *cis*-cyclohexane–, and *trans*-cyclohexane–fused cyclooctenes; and
4. Cycloalkanes-fused cyclooctenes having the lowest RSEs and having RSEs that are lower than or comparable to that of cyclopentene (RSE = 5.2 kcal/mol), including *trans*cyclobutane– and *trans*-cyclopentane–fused cyclooctenes.

The calculated RSEs suggest that the ROMP polymers of the *trans*-cyclobutane– and *trans*-cyclopentane–fused cyclooctenes would undergo catalytic depolymerisation in a way similar to polypentenamers. Because of the synthetic convenience of accessing cyclobutane- and cyclopropane-fused cyclooctenes from 1,5-cyclooctadiene, we employed these cycloalkane-fused cyclooctenes for our experimental and control studies.

Recently, in an effort to control polymer degradation through mechanochemical activation, we synthesized **M1** through a photochemical [2 + 2] cycloaddition of 1,5cyclooctadiene and maleic anhydride followed by $LiAlH_4$ reduction (Fig. 2A)[29]. Note that the cyclobutane in **M1** is *trans*-fused to the

cyclooctene, indicating a *cis*-to-*trans* isomerization of the alkene prior to cycloaddition. Similar inversion of stereochemistry has been observed in other systems[30–33]. Importantly, the moiety of *trans*-cyclobutane-fused cyclooctene (*t*CBCO) is exactly the target moiety we are aiming for. Aside from lactone, *t*CBCOs with other functional groups— including the diesters **M2a** and **M2b**, the diether **M3**, and the imide **M4**—were conveniently derived from the intermediate anhydride **1**.

A high monomer concentration was found to be essential for the ROMP of these monomers, as low monomer concentrations resulted in low conversions. For example, a xylene solution of 1.0 M **M2a** with 1.0 mol% Grubbs' 2nd generation catalyst (**G2**) resulted in 58% conversion when the reaction reached equilibrium at 28 °C. The equilibrium conversion was lowered to 44% when the reaction temperature was raised to 65 °C. From the conversions conducted at various temperatures (Figs. S1–S2), we obtained the thermodynamic data for **M2a** at 1.0 M: $\Delta H = -1.8$ kcal mol^{-1} and $\Delta S = -4.1$ cal mol^{-1} K^{-1}. Similarly, the ΔH (1.0 M) and ΔS (1.0 M) for **M4** we obtained were − 2.2 kcal mol^{-1} and − 3.3 cal mol^{-1} K^{-1}, respectively. While the experimental enthalpy changes confirmed the predicted low RSEs for these monomers, the experimental values are ~ 3 kcal/mol lower than the calculated ones (which are 5.0 kcal/mol and 5.1 kcal/mol for **M2a** and **M4**, respectively). The discrepancy could be due to the presence of other higher-energy conformations in the polymers while the RSEs were calculated using the energies of the most stable conformations. In addition, the entropy changes for these monomers are significantly lower than that for cyclopentene ($\Delta S = -18.5$ cal mol^{1} K^{-1}). The reduced entropy change can be attributed to the lower loss in translational entropy for the larger-sized monomers and the higher gain in rotational entropy due to the higher number of freed bonds in the 8-membered ring that were attained through the ring-opening reaction.

The monomers were subjected to ROMP conditions with 2.0 M monomer concentration in dichloromethane and **G2** as the initiator, yielding the polymers **P1**, **P2a**, **P2b**, **P3**, and **P4** at high conversions (> 80%) (Fig. 2B). The number average molecular weight M_n, dispersity $Đ$, glass transition temperature T_g, and decomposition temperature T_d (defined as the temperature at which 5% weight loss occurs) for each polymer are shown in Fig. 2B. Polymers with high molecular weights (M_n > 100 kDa) were obtained for all polymers. The high dispersities ($Đ$ > 1.5) are comparable to those for other ROMP polymers of low-strain monomers[22,34]. As stated above, an advantage of the 8-membered cycloalkene is that the *cis*-alkene can be inverted to a *trans*-alkene, which is highly strained and is suitable for living ROMP. We converted **M2a** into E-**M2a** through photoisomerization by following the protocol demonstrated by Royzen *et al*.[35]. A controlled ROMP was conducted by employing the conditions developed by Grubbs and coworkers, where Grubbs' first-generation catalyst (**G1**) and excess triphenylphosphine were used[24]. **P2a'** with high molecular weight and low dispersity (M_n = 94.7 kDa, $Đ$ = 1.23) was obtained at high conversion (> 95%) at when the ROMP was conducted at a monomer concentration of 0.25 M.

To test the capability of depolymerisation, the polymers were dissolved in chloroform ($CHCl_3$) or deuterated chloroform ($CDCl_3$) at a concentration of 25 mM and heated at 50 °C in the presence of

underwent > 90% depolymerisation to form the corresponding

monomers (Table S1), as supported by observations obtained via proton nuclear magnetic resonance (^{1}H NMR, Fig. 3A–3C and Figs. S3–S6) and gel permeation chromatography (GPC, Fig. S7). In addition, the recycled monomer (characterization data shown in Figs. S8–S9) from the depolymerisation of **P2a** was subjected to the ROMP conditions described above and yielded polymers of high molecular weight (M_n = 71 kDa, $Đ$ = 1.53, Figs. S10-11). In contrast, when exposed to the same conditions, polycyclooctene did not depolymerise into cyclooctene (Fig. 3D) despite a reduction in molecular weight (Fig. S12A). Moreover, the ROMP polymers of both *cis*- and *trans*-cyclopropane–fused cyclooctenes at the 5,6-positions (*cisg*DCCCO and *trans-g*DCC-CO) did not depolymerise into the corresponding monomers (Fig. 3E–3F), which is consistent with the high RSEs of these monomers (Fig. 1B). In addition, a 1,9-decadiene with *trans*-cyclobutane installed at its 5,6-positions underwent RCM to form *t*CBCO, when it was refluxed in the presence of **G2** (Fig. S13). In contrast, when the *cis*-cyclobutane diene was subjected to the same conditions, no *cis*-cyclobutane-fused cyclooctene was observed in the mass spectrum, which instead showed a mixture of acyclic and cyclic oligomers (Figs. S15-16). The depolymerisation and RCM studies confirm the computational results that *trans*-cyclobutane significantly reduces the RSE of cyclooctene and highlight the impact of the size and stereochemistry of the fused ring on the RSE of a cyclic molecule.

The finding that the ring strain of cyclooctene is reduced by a highly strained cyclobutane is somewhat counterintuitive. Since the ring strain of a cyclic molecule is the relative energy between the cyclic and an acyclic reference, to understand the impact of the fused rings on the ring strain, we examined the structural difference between the cyclooctenes and the acyclic 1,9-decadienes (the structures of which were obtained for ring strain calculations). The ring strain in an unsubstituted cyclooctene can be attributed to the eclipsing effect[36], and this can be conveniently illustrated in a Newman projection along the C5-C6 bond (Fig. S17). The dihedral angles H5C5C6C7, H6C6C5C4 and H5'C5C6H6' in cyclooctene are 25.8º, 24.6º and 19.4º, respectively, generating substantial torsional strain. The eclipsing effect becomes negligible in the acyclic 1,9-diene, as these angles are all close to 60º. We then looked at the *trans*-cyclobutane-fused cyclooctene, in which the H5' and H6' (of an unsubstituted cyclooctene) are replaced with C5' and C6'. As shown in Fig. S17, the dihedral angles H5C5C6C7, H6C6C5C4 and C5'C5C6C6' in *t*CBCO are 30.8º, 29.2º and 17.7º, respectively. Notably, these dihedral angles remain identical in the corresponding acyclic diene. As a result, the relative energy between *t*CBCO and the corresponding acyclic diene is reduced. As for the *cis*-cyclobutane–fused system, while the torsional strain also exists in the acyclic diene, the dihedral angles are significantly different from those in the cyclic form, indicating that the structure of cyclobutane is distorted from the acyclic to the cyclic olefin. The reduction of ring strain by maintaining the eclipsing effect in the acyclic form is therefore offset by the distortion energy in the case of *cis*-cyclobutane-fused cyclooctene. The compensation between these two effects can be generalized to other cycloalkane-fused cyclooctenes: while the cycloalkanes (from 3- to 6-membered rings) reduce the ring strain by locking the conformation of the acyclic form so that the eclipsing effect is present (Figs. S18-19), the fusion of the two rings (the cycloalkane and cyclooctene) can distort the cycloalkane, which raises the rain strain. As shown in Fig. S20, the RSEs of the [illegible] ell with the distortion of the dihedral angles C4-C5-C5'-C6 and

C7-C6-C6′-C5 from the acyclic diene to cycloalkane-fused cyclooctene. The *trans*-cyclobutane therefore represents an ideal scenario where the torsional strain is maintained in both the cyclic and acyclic forms at a low energy cost.

The mild depolymerisation conditions along with the excellent thermal stability (T_d > 370 ºC) of the *t*CBCO polymers make them appealing for use as sustainable materials. Since a wide range of T_g's (from − 30 ºC to 100 ºC) can be accessed through functionalization of *t*CBCO polymers (Fig. 2B), both elastomers and plastics can be prepared. Using the monomer **M2b** (T_g of **P2b** is − 31 ºC) and a *t*CBCO crosslinker **XL1** (Supplementary Information), we prepared an elastomer **PN1** and conducted a tensile test (Fig. 4A). The stress–strain curve showed an elastic deformation up to 50% strain with a Young's modulus of 0.3 MPa, followed by yielding during 50–100% strain and strain hardening from 100% strain, until the maximum strain was reached at ~ 200% strain. Previous work by Moore and coworkers has shown that metathesis-based depolymerisation can occur in bulk materials, suggesting that the crosslinked material here should still be depolymerisable[37]. 94% depolymerisation was observed when **PN1** was immersed in a solution of **G2** in $CDCl_3$ and was heated to 50 ºC for 2 h (Fig. S21).

The imide-functionalized *t*CBCO polymer **P4** has a T_g of 100 ºC (Fig. 2B), comparable to that of polystyrene, which is one of the most widely used plastics. The large thermal processing window (which is above the T_g but below the T_d) of **P4** allowed the melt-pressing of films of the material. From the melt-pressed film of **P4**, we prepared a dogbone specimen and conducted tensile testing to obtain the stress–strain curve (Fig. 4B). A polystyrene sample was processed in the same manner and was subjected to tensile testing for comparison. As shown in Fig. 4B, P4 showed a Young's modulus of 3.0 ± 0.5 GPa, which is comparable to that of polystyrene. The strain at break (8 ± 0.5%) and the tensile strength (4.0 ± 0.6 MPa) were higher than those of polystyrene (strain at break of 6 ± 0.5% and a tensile strength of 2.0 ± 0.5 MPa).

In principle, the *t*CBCO monomers can be obtained by the photochemical [2 + 2] cycloaddition of 1,5-cyclooctadiene with any olefins, therefore providing numerous possibilities of functionality and material properties. Since 1,5-cyclooctadiene can be prepared from the dimerization of butadiene (a starting material for synthetic rubbers) and since olefins are the starting materials for plastics, it will therefore be relatively convenient to produce the chemically recyclable *t*CBCO polymers based on current practices in the rubber and plastics industries. The concept of controlling ring strain using an additional ring—as well as the insights gained in this study on how the size and stereochemistry of the fused ring impact the ring strain—can be useful for many other fields where ring strain plays an important role, including mechanochemistry[38], molecular machines[39], catalysis[40] and click chemistry[41].

Methods

A complete set of detailed synthetic procedures for monomers and polymers along with their spectral data is available in Supplementary Information.

Materials and instrumentation. *Cis*-2-Butene-1,4-diol, acetic anhydride and 2,2-dimethoxypropane were purchased from Alfa Aesar. *(Z,Z)*-1,5-cyclooctadiene, *N*-phenylmaleimide, methyltriphenylphosphonium bromide, potassium *tert*-butoxide, sodium acetate and aniline were purchased from TCI. Grubbs 1st and 2nd generation catalysts, benzophenone, lithium aluminum hydride, *p*-toluenesulfonic acid, 1,4-butanediol, ethyl vinyl ether, Quadrapure TU, sodium periodate, sodium hydride, methyl benzoate, methyl iodide and cuprous iodide were purchased from Sigma Aldrich. Maleic anhydride, 3-chloroperoxybenzoic acid, *p*-toluenesulfonyl chloride, sodium borohydride, triethylamine, acetic acid, silver nitrate and allylmagnesium chloride (1.7 M solution in THF) were purchased from Acros Organics. Polystyrene (Styron 663) was obtained from Dow. Unless specified, all reagents were used as received without further purification. Column chromatography was performed using Silicycle F60 (230–400 mesh) silica gel.

LaboACE LC-5060 preparatory GPC with two JAIGEL-2HR columns was used for purification where specified, with HPLC grade chloroform containing 0.75% ethanol as the eluent.

^{1}H NMR and ^{13}C NMR spectra were obtained on either a Varian 300 or a 500 MHz spectrometer with $CDCl_3$ or acetone-d_6 as the solvents. Single crystal data for all structures were collected on a Bruker CCD-based diffractometer with dual Cu/Mo ImuS microfocus optics (Cu Kα radiation, λ = 1.54178 Å or Mo Kα radiation, λ = 0.71073). Crystals were mounted on a cryoloop using Paratone oil and placed under a steam of nitrogen at 100 K (Oxford Cryosystems). The data were corrected for absorption with the SADABS program. The structures were refined using Bruker SHELXTL Software Package (Version 6.1) and were solved using direct methods until the final anisotropic full-matrix least squares refinement of F2 converged. Electronic Supplementary Information (ESI) available: CCDC 2032007–2032009 contains the supplementary crystallographic data for this paper. These data can be obtained free of charge from The Cambridge Crystallographic Data Centre via www.ccdc.cam.ac.uk/data_request/cif.

High resolution mass spectra (HRMS) were performed on Waters Synapt HDMS Quadrupole/Time-of-Flight (Q-ToF) Mass Spectrometer (Waters, Beverly, MA) in positive ion mode.

Gel permeation chromatography (GPC) was carried out with a Tosoh EcoSEC HLC-8320GPC Quad Detector with two 17393 TSKgel columns (7.8 mm ID x 30 cm, 13 μm) and one 17367-TSKgel Guard Column (7.5 mm ID x 7.5 cm, 13 μm).

Thermal properties were determined using a TA Discovery DSC 250 and TGA 550. Tensile testing was performed using an Instron 5969 tensile tester or using a home-built tensile tester with a 10 kg load cell controlled by an Arduino UNO.

Calculations of ring strain energies. The ring strain energies of the cyclic olefins were calculated by following a method demonstrated by Grubbs and coworkers (22). This method involves the calculation of the enthalpy change for the ring-closing metathesis (Eq. 1). Since the numbers and types of bonds of the reactant are identical to those of the products (i.e., an isodesmic reaction), the enthalpy change of the reaction should come solely from the change in ring strain (Eq. 2)—which is essentially the ring strain of the acyclic diene reactant or the ethylene product.

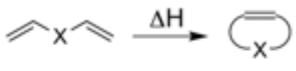

(1)

$$RSE = \Delta H = H_{ethene} + H_{cyclic\ olefin} - H_{diene} \quad (2)$$

All calculations were performed using Gaussian 16 at the B3LYP/6-31G(d,p) level of theory. The structures were first optimized with a UFF forcefield as implemented in the auto-optimization tool in Avogadro, followed by a conformer search with Avogadro, and the optimized conformation was subjected to geometry optimization and vibrational frequency calculations with Gaussian 16.

Thermodynamic Studies of Polymerization. Thermodynamic studies were performed for the diester monomer M2a and imide monomer M4. The polymerization for each monomer was conducted at 5 different temperatures and the equilibrium monomer concentration $[M]_e$ for each temperature was measured via ^{1}H NMR. The thermodynamic parameters were obtained by plotting $\ln[M]_e$ against temperature 1/T (van't Hoff plot) according to Eq. 3.

$$ln\ [M]_e = \frac{\Delta H}{RT} - \frac{\Delta S}{R} \quad (3)$$

In Eq. 3, $[M]_e$ is the equilibrium monomer concentration in mol.L^{-1}, T is the reaction temperature in Kelvin (K), ΔH is the enthalpy of reaction in kcal mol^{-1}, ΔS is the entropy of reaction in kcal mol^{-1} K^{-1}. ΔH and ΔS can be obtained from the slope and the intercept of the van't Hoff plot, respectively. The following procedure is a representative example of the polymerization performed here.

M2a (250 mg, 0.998 mmol, 1 eq.) was added to a vial with a small stir bar and dissolved in xylene (998 µL), such that initial monomer concentration was 1M. **G2** (8.41 mg, 0.00998 mmol, 0.01 eq.) was added to the monomer solution. 200 µL of the solution was added to each of another four vials, and the five vials were placed in an oil bath that was pre-heated to the desired temperatures. After 7 h, the reactions were quenched with ethyl vinyl ether (50 µL) and the conversion was measured with ^{1}H NMR. Fig. S1 and Fig. S2 contain the equilibrium monomer concentration for polymerization of **M2a** and **M4** at various temperatures (averaged over three runs), respectively.

Comparison of the integration of the monomer and polymer olefinic peaks in the ^{1}H NMR spectra (Fig. S67) was used to determine residual monomer content at equilibrium. The monomer olefinic peak appears resolved from the polymer olefinic peak and has a shift downfield of it.

From the van't Hoff plot for **M2a** (Fig. S1), the slope was obtained to be -878.3138 and the intercept n were calculated as below:

$$\frac{\Delta H}{R} = -878.3138$$

$$-\frac{\Delta S}{R} = 2.0345$$

This gave ΔH = -1.8 kcal.mol^{-1} and ΔS = -4.1 cal.mol^{-1}.K^{-1}. Similarly, ΔH = -2.2 kcal.mol^{-1} and ΔS = -3.3 cal.mol^{-1}.K^{-1} were obtained for **M4** (Fig. S2).

Depolymerisation studies. A representative depolymerisation procedure is shown in the following: in a vial equipped with a stir bar, **P2a (**146.5 mg, 0.58 mmol, 1 eq.) was dissolved in $CHCl_3$ (5 mL). To the polymer solution was added **G2** (4.93 mg, 0.0058 mmol, 0.01 eq.) from a stock solution. The volume of the added **G2** solution was pre-calculated to obtain a concentration of 100 mM for the olefin groups. The vial was placed in an oil bath preheated to 50 ^{o}C and stirred for 2 hours. 0.5 mL ethyl vinyl ether was added to quench the reaction and the mixture was allowed to stir for 15 min. The vial was allowed to cool down to room temperature, and 930 mg of Quadrapure TU macroporous particles and 1 mL $CHCl_3$ were added. The mixture was allowed to stir overnight followed by filtration through a Celite plug. The filtrate was concentrated on a rotavap and characterized with ^{1}H NMR and GPC. Initial molecular weight and concentration, as well as extent of conversion to monomer for each polymer are shown in Table S1.

Mechanical Testing. For tensile testing of **P4**, a DCM solution was the polymer was allowed to dry under ambient conditions followed by drying in a vacuum oven at 110-120 ^{o}C for 2 days until there was no further mass change. Dogbone-shaped samples of gauge length 10 × 3 × 1.5 mm^3 were prepared by compression molding using a Carver Lab Press at 0 kg pressure for 3 minutes at 130-150 ^{o}C, followed by 9000 kg pressure for 5 min at the same temperature. Samples were then quenched in water, and allowed to equilibrate for an hour at room temperature prior to examination of the mechanical properties. Dogbone samples of polystyrene acquired from Dow (Styron 663) were obtained by similar procedure, for comparison. Mechanical properties were determined at constant speed V = 5 mm/min with a 5969 tensile tester from Instron. Since the initial length was 10 mm, the initial crosshead speed V/L_0 was 0.5 min^{-1}.

Tensile testing of the elastomer sample **PN1** was performed on a home-built tensile tester controlled by an Arduino UNO board. A crosshead speed of 5 mm/min was used.

Declarations

Acknowledgements: This work is supported by The University of Akron. The computational resources were provided by XSEDE (TG-CHE190099). The single-crystal structures were characterized with an X-ray diffractometer supported by the National Science Foundation (CHE-0840446). We thank S. Wang for helpful discussion and thank K. Williams-Pavlantos and C. Wesdemiotis for conducting mass spectrometry analysis.

Author Contributions: J.W. conceived the project and directed the research. D.S. and J.W. performed the DFT calculations and analyzed the computational data. D.S., J.Z., H.C., W.X., H-W.S. and T-G.H. conducted monomer and polymer synthesis. B.R.S. and C.J.Z. collected and analyzed the single-crystal data. D.S. and W.X. conducted thermodynamic studies and depolymerisation. J.Z. conducted ring-closing metathesis experiments. D.S. and J.Z. conducted thermal characterization of the polymers. D.S. and T.S. conducted mechanical testing. D.S. and J.W. prepared the manuscript.

Author Information Reprints and permissions information is available at www.nature.com/reprints. The authors declare no competing financial interests. Correspondence and requests for materials should be addressed to J.W. (jwang6@uakron.edu).

References

1 Rochman, C. M. *et al.* Classify plastic waste as hazardous. *Nature* **494**, 169-171, (2013).

2 Foundation, E. M. The new plastics economy: Rethinking the future of plastics & catalysing action., (2017).

3 Haider, T. P., Völker, C., Kramm, J., Landfester, K. & Wurm, F. R. Plastics of the future? The impact of biodegradable polymers on the environment and on society. *Angew. Chem. Int. Ed.* **58**, 50-62, (2019).

4 Ignatyev, I. A., Thielemans, W. & Vander Beke, B. Recycling of polymers: A review. *ChemSusChem* **7**, 1579-1593, (2014).

5 Tang, X. & Chen, E. Y. X. Toward infinitely recyclable plastics derived from renewable cyclic esters. *Chem* **5**, 284-312, (2019).

6 Coates, G. W. & Getzler, Y. D. Y. L. Chemical recycling to monomer for an ideal, circular polymer economy. *Nat. Rev. Mater.* **5**, 501-516, (2020).

7 Snow, R. D. & Frey, F. E. The reaction of sulfur dioxide with olefins: The ceiling temperature phenomenon. *J. Am. Chem. Soc.* **65**, 2417-2418, (1943).

8 Dainton, F. S. & Ivin, K. J. Reversibility of the propagation reaction in polymerization processes and its manifestation in the phenomenon of a ‘ceiling temperature'. *Nature* **162**, 705-707, (1948).

9 McCormick, H. W. Ceiling temperature of α-methylstyrene. *J. Polym. Sci.* **25**, 488-490, (1957).

10 North, A. M. & Richardson, D. Entropy of stereoregularity in aldehyde polymerization. *Polymer* **6**, 333-338, (1965).

11 Park, C. W. *et al.* Thermally triggered degradation of transient electronic devices. *Adv. Mater.* **27**, 3783-3788, (2015).

12 Feinberg, A. M. *et al.* Cyclic poly(phthalaldehyde): Thermoforming a bulk transient material. *ACS Macro Lett.* **7**, 47-52, (2018).

13 Tran, H. *et al.* Stretchable and fully degradable semiconductors for transient electronics. *ACS Cent. Sci.* **5**, 1884-1891, (2019).

14 Zhu, J.-B., Watson, E. M., Tang, J. & Chen, E. Y. X. A synthetic polymer system with repeatable chemical recyclability. *Science* **360**, 398, (2018).

15 Grubbs, R. H. Olefin metathesis. *Tetrahedron* **60**, 7117-7140, (2004).

16 Grubbs, R. H. & Khosravi, E. *Handbook of metathesis: Polymer synthesis*. 2nd edn, Vol. 3 (2015).

17 Monfette, S. & Fogg, D. E. Equilibrium ring-closing metathesis. *Chem. Rev.* **109**, 3783-3816, (2009).

18 Neary, W. J. & Kennemur, J. G. Polypentenamer renaissance: Challenges and opportunities. *ACS Macro Lett.* **8**, 46-56, (2019).

19 Myers, S. B. & Register, R. A. Synthesis of narrow-distribution polycyclopentene using a ruthenium ring-opening metathesis initiator. *Polymer* **49**, 877-882, (2008).

20 Neary, W. J. & Kennemur, J. G. Variable temperature romp: Leveraging low ring strain thermodynamics to achieve well-defined polypentenamers. *Macromolecules* **50**, 4935-4941, (2017).

21 Schleyer, P. v. R., Williams, J. E. & Blanchard, K. R. Evaluation of strain in hydrocarbons. The strain in adamantane and its origin. *J. Am. Chem. Soc.* **92**, 2377-2386, (1970).

22 Hejl, A., Scherman, O. A. & Grubbs, R. H. Ring-opening metathesis polymerization of functionalized low-strain monomers with ruthenium-based catalysts. *Macromolecules* **38**, 7214-7218, (2005).

23 Martinez, H., Ren, N., Matta, M. E. & Hillmyer, M. A. Ring-opening metathesis polymerization of 8-membered cyclic olefins. *Polym. Chem.* **5**, 3507-3532, (2014).

24 Walker, R., Conrad, R. M. & Grubbs, R. H. The living romp of trans-cyclooctene. *Macromolecules* **42**, 599-605, (2009).

25 You, W., Padgett, E., MacMillan, S. N., Muller, D. A. & Coates, G. W. Highly conductive and chemically stable alkaline anion exchange membranes via romp of trans-cyclooctene derivatives. *Proc. Natl. Acad. Sci. U. S. A.* **116**, 9729, (2019).

26 Since different ring strain energies have been reported for cyclooctene, we use our calculated values throughout the text for consistency.

27 You, W., Hugar, K. M. & Coates, G. W. Synthesis of alkaline anion exchange membranes with chemically stable imidazolium cations: Unexpected cross-linked macrocycles from ring-fused romp monomers. *Macromolecules* **51**, 3212-3218, (2018).

28 Scherman, O. A., Walker, R. & Grubbs, R. H. Synthesis and characterization of stereoregular ethylene-vinyl alcohol copolymers made by ring-opening metathesis polymerization. *Macromolecules* **38**, 9009-9014, (2005).

29 Hsu, T.-G. *et al.* A polymer with “locked” degradability: Superior backbone stability and accessible degradability enabled by mechanophore installation. *J. Am. Chem. Soc.* **142**, 2100-2104, (2020).

30 Asaoka, S., Horiguchi, H., Wada, T. & Inoue, Y. Enantiodifferentiating photocyclodimerization of cyclohexene sensitized by chiral benzenecarboxylates. *J. Chem. Soc., Perkin Trans. 2*, 737-747, (2000).

31 Maeda, H. *et al.* Synthesis and photochemical properties of stilbenophanes tethered by silyl chains. Control of (2π + 2π) photocycloaddition, cis−trans photoisomerization, and photocyclization. *J. Org. Chem.* **70**, 9693-9701, (2005).

32 Xu, Y., Smith, M. D., Krause, J. A. & Shimizu, L. S. Control of the intramolecular [2+2] photocycloaddition in a bis-stilbene macrocycle. *J. Org. Chem.* **74**, 4874-4877, (2009).

33 Poplata, S., Tröster, A., Zou, Y.-Q. & Bach, T. Recent advances in the synthesis of cyclobutanes by olefin [2+2] photocycloaddition reactions. *Chem. Rev.* **116**, 9748-9815, (2016).

34 Feist, J. D. & Xia, Y. Enol ethers are effective monomers for ring-opening metathesis polymerization: Synthesis of degradable and depolymerisable poly(2,3-dihydrofuran). *J. Am. Chem. Soc.* **142**, 1186-1189, (2020).

35 Royzen, M., Yap, G. P. A. & Fox, J. M. A photochemical synthesis of functionalized trans-cyclooctenes driven by metal complexation. *J. Am. Chem. Soc.* **130**, 3760-3761, (2008).

36 Bach, R. D. Ring strain energy in the cyclooctyl system. The effect of strain energy on [3 + 2] cycloaddition reactions with azides. *J. Am. Chem. Soc.* **131**, 5233-5243, (2009).

37 Liu, H. *et al.* Dynamic remodeling of covalent networks via ring-opening metathesis polymerization. *ACS Macro Lett.* **7**, 933-937, (2018).

38 Caruso, M. M. *et al.* Mechanically-induced chemical changes in polymeric materials. *Chem. Rev.* **109**, 5755-5798, (2009).

39 Feringa, B. L. The art of building small: From molecular switches to motors (nobel lecture). *Angew. Chem. Int. Ed.* **56**, 11060-11078, (2017).

40 Walczak, M. A. A., Krainz, T. & Wipf, P. Ring-strain-enabled reaction discovery: New heterocycles from bicyclo[1.1.0]butanes. *Acc. Chem. Res.* **48**, 1149-1158, (2015).

41 Agard, N. J., Prescher, J. A. & Bertozzi, C. R. A strain-promoted [3 + 2] azide–alkyne cycloaddition for covalent modification of biomolecules in living systems. *J. Am. Chem. Soc.* **126**, 15046-15047, (2004).

Figures

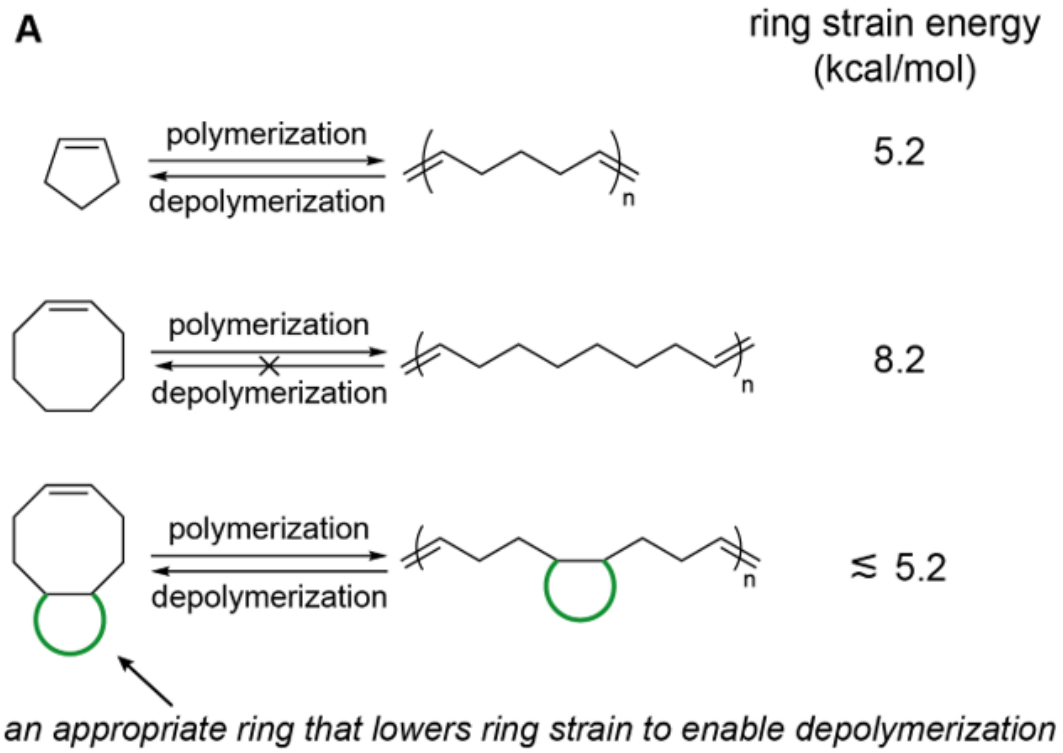

B

	3-mem	*4-mem*	*5-mem*	*6-mem*
cis	9.8	10.3	7.6	7.2
trans	10.3	4.9	5.3	7.5

Figure 1

Identifying the appropriate ring that lowers the ring strain energy for cyclooctene to enable depolymerisation of the corresponding polymer. (A) Polycyclopentene is depolymerisable whereas polycyclooctene is not. The difference is caused by a higher ring strain energy in cyclooctene. An appropriate fused ring lowers the ring strain energy of cyclooctene to a level that is comparable to that of the polymer. (B) The calculated ring strain energies (shown in

kcal/mol) for cyclooctene with 3-, 4-, 5- and 6-membered rings both cis- and trans-fused at the 5,6-positions.

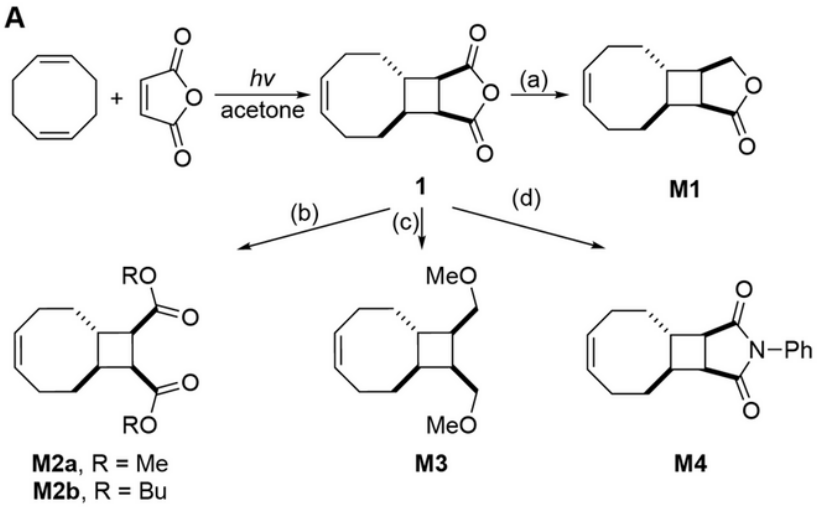

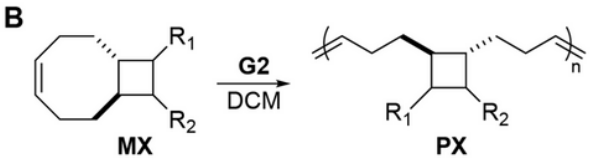

	M_n (kDa)	$Đ$	T_d (ºC)	T_g (ºC)
P1	105	1.42	430	49
P2a	142	1.55	401	18
P2b	124	1.93	370	-31
P3	293	1.91	372	-34
P4	198	1.96	409	100

Figure 2

Synthesis and characterization. (A) Synthetic scheme of the trans-cyclobutane-fused cyclooctene (tCBCO) monomers. Photochemical [2+2] cycloaddition of 1,5-cyclooctadiene and maleic anhydride affords the anhydride 1, which can be readily converted to M1, M2, M3 and M4 through conditions (a), (b), (c) and (d), respectively. (a) 0.5 eq LiAlH4, THF. (b) ROH, heating, cat. H+. (c) 1.0 eq LiAlH4, THF; NaH, MeI, THF. (d) Aniline, acetone; sodium acetate, acetic anhydride, 100 ºC. (B) Synthetic scheme, molecular weight information and thermal characterization data of the tCBCO polymers.

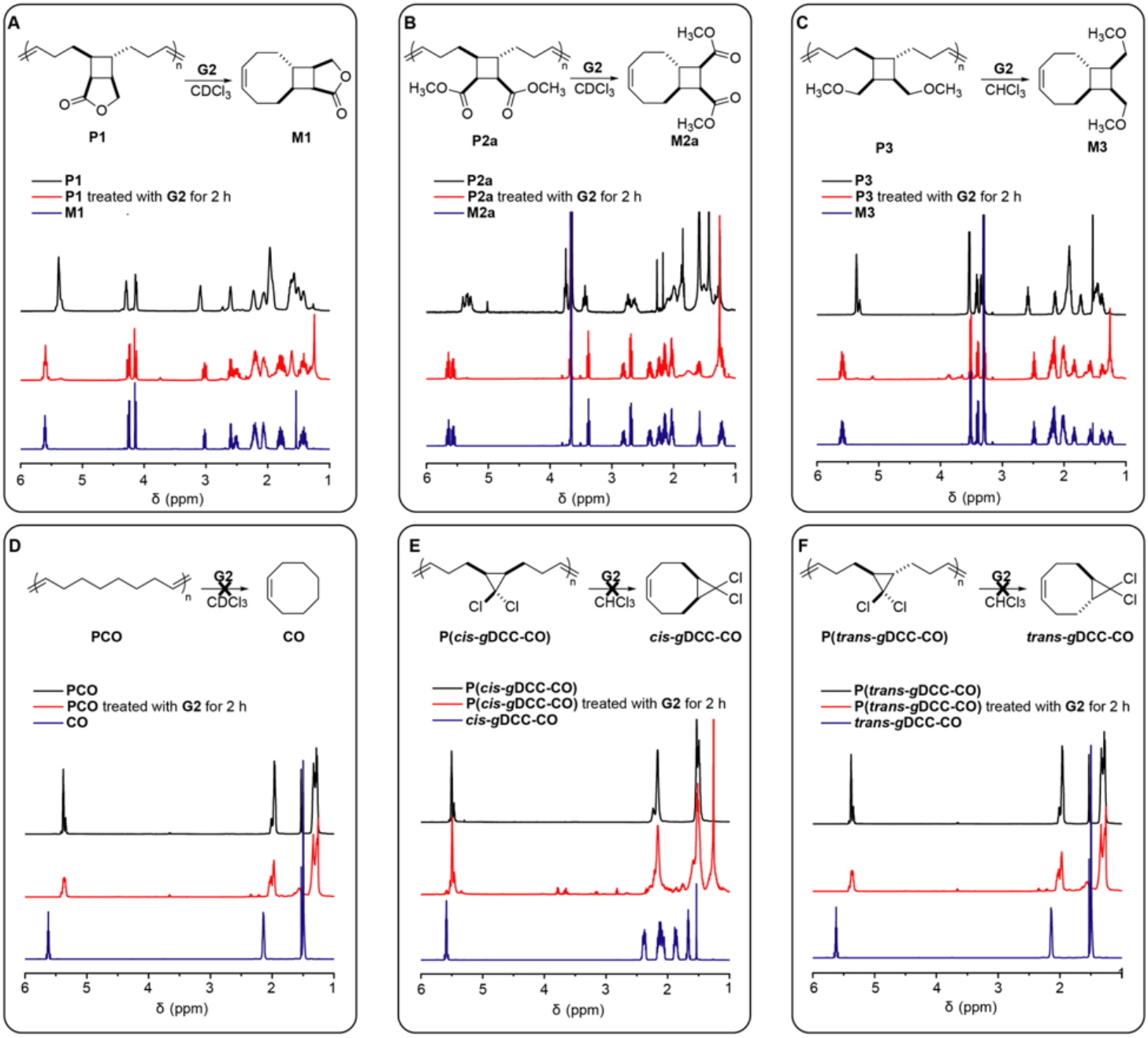

Figure 3

Depolymerisation studies. The 1H NMR spectra for P1 (A), P2a (B), P3 (C), polycyclooctene (D), poly(cis-gDCC-CO) (E), poly(trans-gDCC-CO) (F) before (in black) and after (in red) 2 h of heating at 50 °C in the presence of G2. The 1H NMR spectra of the corresponding monomers are shown (in blue) as references.

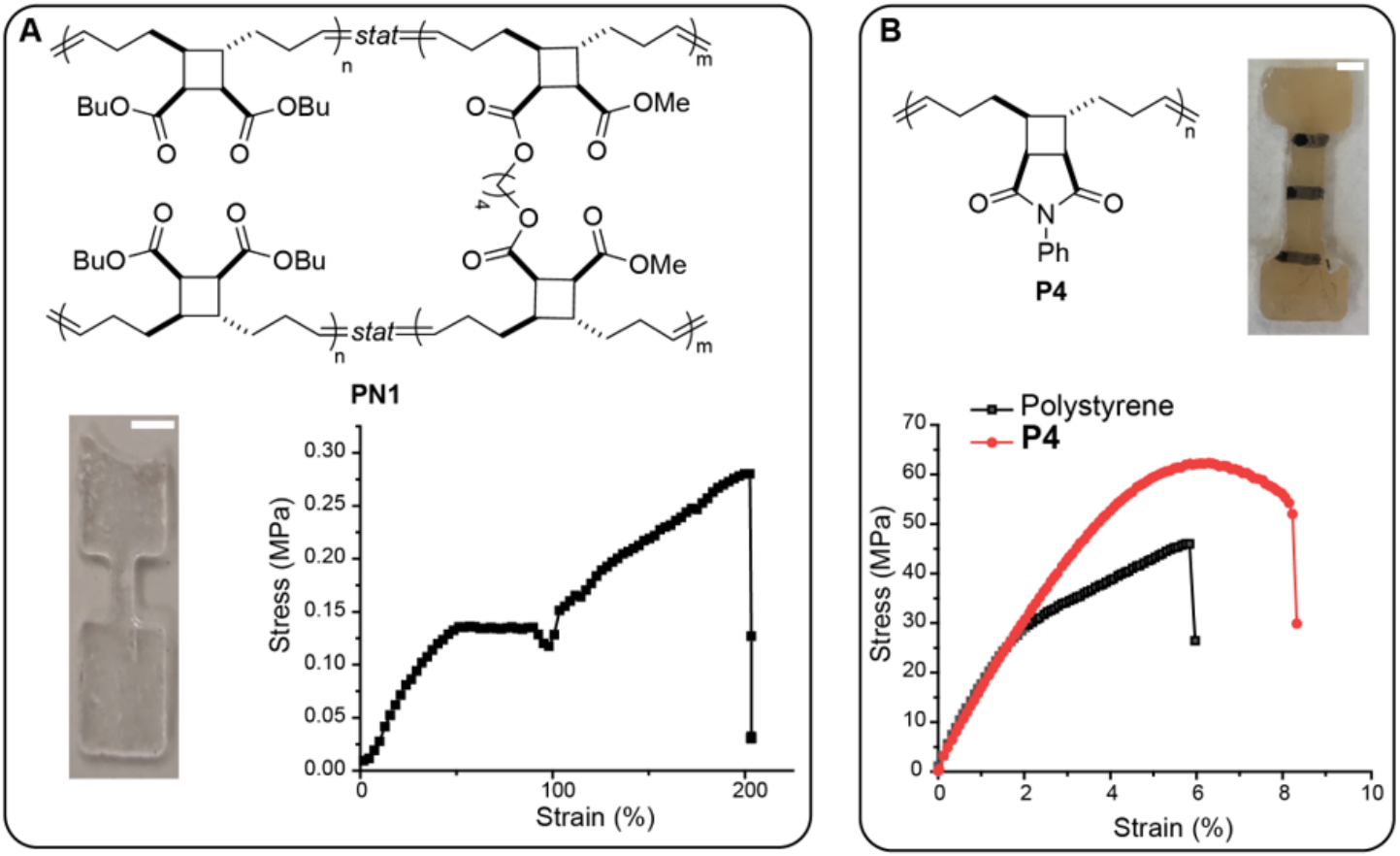

Figure 4

Mechanical properties. (A) Chemical structure of the tCBCO-based elastomer PN1, a photo of the dogbone specimen of PN1 (scale bar: 2 mm) and stress–strain curve obtained from the tensile test (5 mm/min, room temperature) for PN1. (B) Chemical structure of the glassy polymer P4, a photo of dogbone specimen (scale bar: 2 mm) of P4, and stress–strain curves for P4 (in red) and polystyrene (in black) obtained from tensile test (5 mm/min, room temperature).

Supplementary Files

This is a list of supplementary files associated with this preprint. Click to download.

- ChemicallyrecyclablepolymerSIfinal.pdf
- compound2.cif
- compound6.cif
- compound10.cif